

NANO EXPRESS

Open Access



Effect of Oblique-Angle Sputtered ITO Electrode in MAPbI₃ Perovskite Solar Cell Structures

Kun-Yi Lee¹, Lung-Chien Chen^{2*}  and Yu-June Wu³

Abstract

This investigation reports on the characteristics of MAPbI₃ perovskite films on obliquely sputtered ITO/glass substrates that are fabricated with various sputtering times and sputtering angles. The grain size of a MAPbI₃ perovskite film increases with the oblique sputtering angle of ITO thin films from 0° to 80°, indicating that the surface properties of the ITO affect the wettability of the PEDOT:PSS thin film and thereby dominates the number of perovskite nucleation sites. The optimal power conversion efficiency (Eff) is achieved 11.3% in a cell with an oblique ITO layer that was prepared using a sputtering angle of 30° for a sputtering time of 15 min.

Keywords: Oblique-angle sputtered ITO, MAPbI₃ perovskite, Wettability

Background

Indium tin oxide (ITO) is a transparent conductive material that comprises indium oxide (In₂O₃) and tin oxide (SnO₂). It is widely used in liquid crystal displays, light-emitting diodes, and solar cells owing to its visible transparency of approximately 96% and conductivity of around 10 Ω/sq [1–5]. Several methods for improving the resistance and the transmittance of ITO films have been studied, including annealing and sputtering with various gas ratios and operating pressures [5–8]. The optoelectronic properties of obliquely sputtered ITO films have been reported upon [9, 10]. As an ITO film is deposited, it grows as a film with a tilted columnar structure at an angle on a substrate, owing to the shadow effect. The columnar ITO film exhibits a different morphology, anisotropic optical properties, and anisotropic resistivity [10].

Recently, solar cells with perovskite materials, such as CH₃NH₃PbI₃, as an active layer have received much interest owing to their favorable power conversion efficiencies [11–18]. Most perovskite solar cells

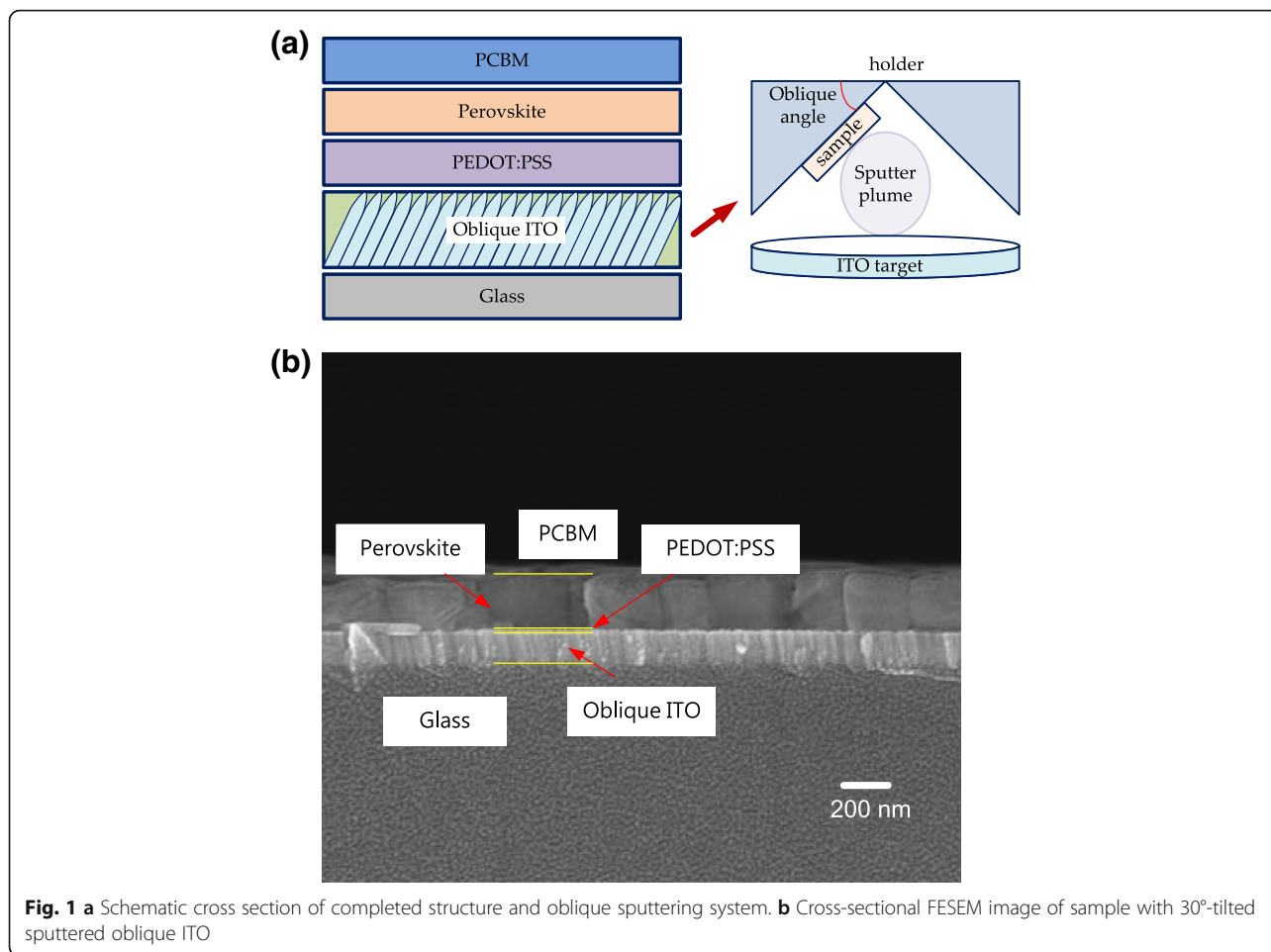
have transparent conductive oxide (TCO) glass, such as ITO or FTO (fluorine-doped tin oxide), as the substrate. However, the optoelectronic properties of an isotropic TCO film differ from those of an anisotropic TCO film. Therefore, this work develops planar perovskite solar cells using CH₃NH₃PbI₃ (MAPbI₃) perovskites on oblique ITO substrates that are prepared glancing angle deposition (GLAD). This investigation examines the optical, structural, and surface properties of MAPbI₃ perovskite films on oblique ITO substrates that have been annealed at various temperatures and sputtered for various times. The relationships between the performance of the perovskite solar cell and the properties of the perovskite films are discussed.

Methods

In this investigation, ITO glass was cut into small pieces of size 1.5 × 1.5 cm² be used as substrates. The ITO glass substrates were thoroughly cleaned using acetone, ethanol, and deionized (DI) water in an ultrasonic oscillator for 5 min and dried with nitrogen. An ITO film was deposited onto the ITO glass substrate by sputtering at various oblique angles using ITO targets, as presented in Fig. 1a. The working gas and

* Correspondence: ocean@ntut.edu.tw

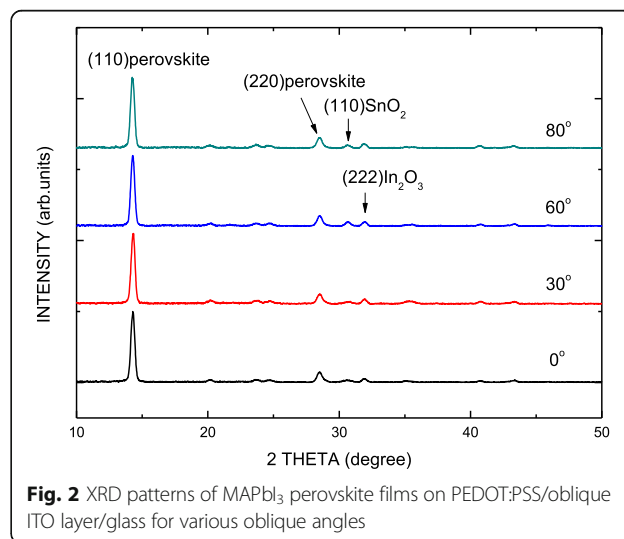
²Department of Electro-optical Engineering, National Taipei University of Technology, 1, 3 Sec., Chung-Hsiao E. Rd, Taipei 106, Taiwan
Full list of author information is available at the end of the article



pressure were pure argon and 5 mTorr, respectively. After deposition, the films were annealed at 300 °C for 30 min.

Glass substrates that were coated with the obliquely sputtered ITO films were used for the perovskite solar cells. PEDOT:PSS films were prepared by spin-coating the oblique ITO glass substrates at 5000 rpm for 30 s. After spin-coating, the film was annealed at 110 °C for 10 min. The perovskite layer was deposited using two-step spin-coating onto the PEDOT:PSS/oblique ITO glass substrate at 1000 rpm for 10 s and 5000 rpm for 20 s. During the step at 5000 rpm for 20 s, the wet spinning film was quenched by dropping 100 µl of anhydrous toluene onto it. The perovskite precursor solutions were prepared using 1.25 mmol methylammonium bromide and 1.25 mmol PbI₂ (with a purity of 99.999%) that was dissolved in 1 mL cosolvent. The volume ratio of dimethyl sulfoxide (DMSO) to γ-butyrolactone (GBL) was 1:1. After spin-coating, the film was annealed at 100 °C for 10 min. Then [6,6]-phenyl-C₆₁-butyric acid methyl ester (PCBM) was dissolved in chlorobenzene (20 mg/mL) and spin-coated on perovskite layers at 3000 rpm for 30 s, forming a 50-nm-thick film as an electron transport layer. Finally, an

Ag electrode with a thickness of 20 nm was deposited by thermal evaporation to complete the structure of the device. The sample was covered with a shadow mask that defined an active area of 0.5 cm × 0.2 cm during the deposition. Figure 1a schematically depicts the complete



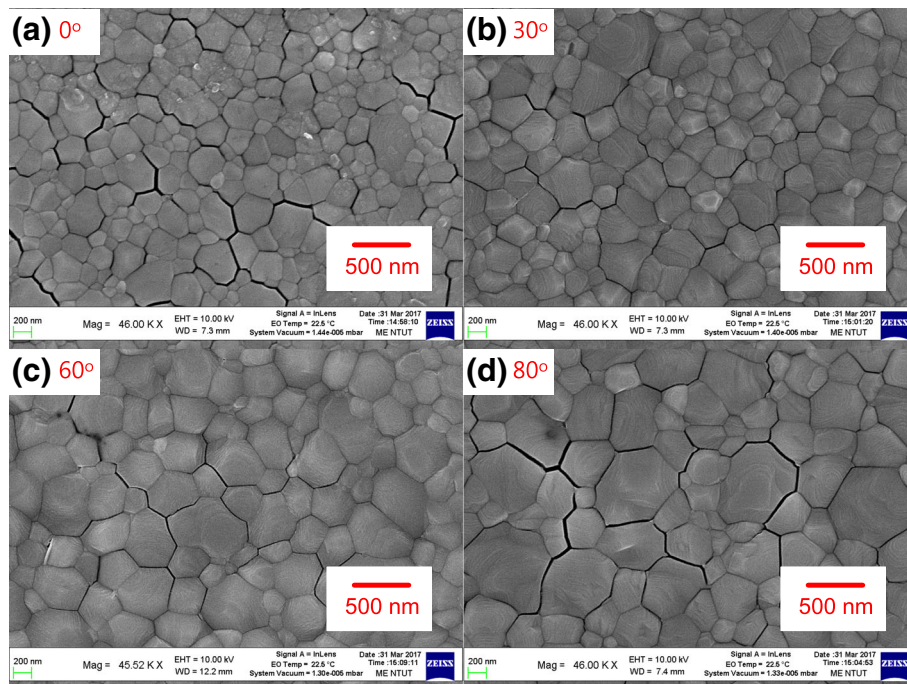


Fig. 3 a-d SEM images of MAPbI₃ perovskite films on PEDOT:PSS/oblique ITO layer/glass for various oblique angles

structure. Figure 1b shows the cross-sectional FESEM image of the sample with the 30°-tilted obliquely sputtered ITO.

Results and Discussion

The crystalline microstructures of the films were observed using an X-ray diffractometer. A field-emission scanning electron microscope (FESEM) was used to observe the surface morphology of the samples. The current density–voltage (*J–V*) characteristics of the solar cells were measured using a Keithley 2420 programmable source meter under irradiation by a 1000 W xenon lamp. The irradiation power density on the surface of the cell was calibrated to 1000 W/m².

Figure 2 shows the XRD patterns of the MAPbI₃ perovskite films on PEDOT:PSS/oblique ITO layer/glass at various oblique angles. The four mean peaks at 14.28°, 28.5°, 30.61°, and 31.93° correspond to the (110) perovskite, (220) perovskite, (110) SnO₂, and (222) In₂O₃ planes, respectively. As the sputtering angle increases from 0° to 60°, the (110) SnO₂ is formed by the incorporation of Sn atoms. The size of the crystal domain can be calculated using Scherrer’s equation [19]. The sizes of the crystal domains of the MAPbI₃ perovskite films in the samples are approximately 71.8 nm. Therefore, the sizes of the crystal domains of the MAPbI₃ perovskite are not affected by the oblique ITO layer.

Figure 3 shows SEM images of MAPbI₃ perovskite films on an oblique ITO layer/glass for various oblique angles.

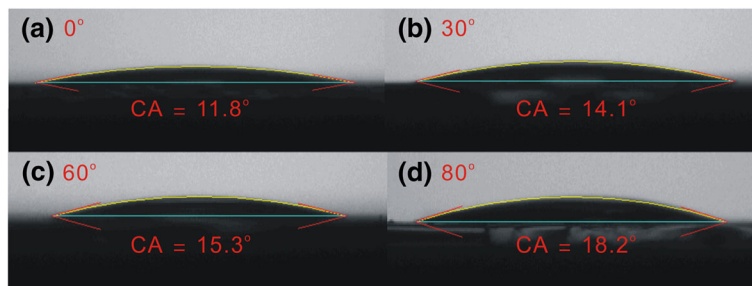


Fig. 4 a-d Images that show contact angle of water on PEDOT:PSS/oblique ITO layer/glass for various oblique angles. CA contact angle

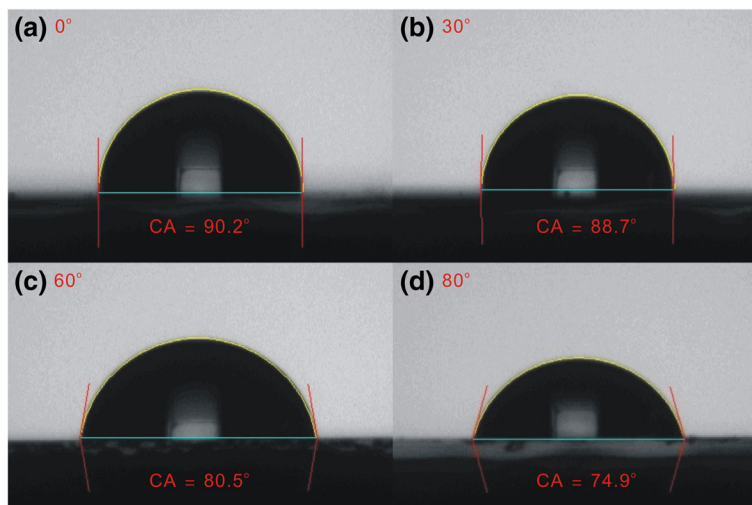


Fig. 5 a-d Images that show contact angle of water on oblique ITO layer/glass for various oblique angles

The grain (or particle) size of the MAPbI₃ perovskite films increases with the oblique sputtering angle from 0° to 80°, revealing that the surface properties of the ITO influence the number of perovskite nucleation sites. Since the ITO is not in direct contact with the perovskite thin film and a PEDOT:PSS thin film is inserted between the ITO and the perovskite, the surface properties of the ITO should not directly influence the properties of the perovskite thin films. Hence, the wettability of the PEDOT:PSS thin films [20] is related to the surface properties of the ITO. Therefore, the different grain sizes in the MAPbI₃ perovskite films may be related to the wettability of the substrate [21, 22]. Experiments on the contact angle of a water droplet were carried out to assess the wettability of the PEDOT:PSS thin films

on the different ITO/glass samples, as shown in Fig. 4. The contact angle is proportional to the size of the grains in the MAPbI₃ thin film, indicating that the nucleation and crystal growth of a MAPbI₃ thin film can be controlled by varying the surface wettability of the PEDOT:PSS/oblique ITO/glass. Contact angle images of the oblique ITO/glass samples were obtained to understand the variation of the surface wettability of the PEDOT:PSS/oblique ITO/glass samples, as depicted in Fig. 5. The wettability of the PEDOT:PSS/oblique ITO/glass samples is inversely proportional to the wettability of the oblique ITO/glass samples, so the vertical distributions of the hydrophilic PSS polymers and hydrophobic PEDOT polymers can be manipulated by varying the surface wettability of the oblique ITO/glass sample. PSS polymers are suggested to be distributed mostly in the upper surface of the PEDOT:PSS thin film when the substrate has a hydrophobic surface (Fig. 5a), resulting in a small water droplet contact angle on the PEDOT:PSS thin film (Fig. 4a). The experimental results (XRD and SEM) demonstrate that the MAPbI₃ grains are multi-crystalline MAPbI₃ particles [23].

Figure 6 presents the photoluminescence (PL) spectra of the MAPbI₃ perovskite films on PEDOT:PSS/oblique ITO/glass for various oblique angles. One main peak is observed at 768 nm, corresponding to emission by MAPbI₃. The finding is supported by the XRD results. The PL emission energy of the MAPbI₃ perovskite is not affected from beneath the oblique ITO layer. Additionally, the different PL intensities of the MAPbI₃ films on ITOs sputtered with various oblique angles were obtained as a result of the separation of the light-induced exciton. A better interface between PEDOT:PSS and perovskite provided better exciton separation, inducing a

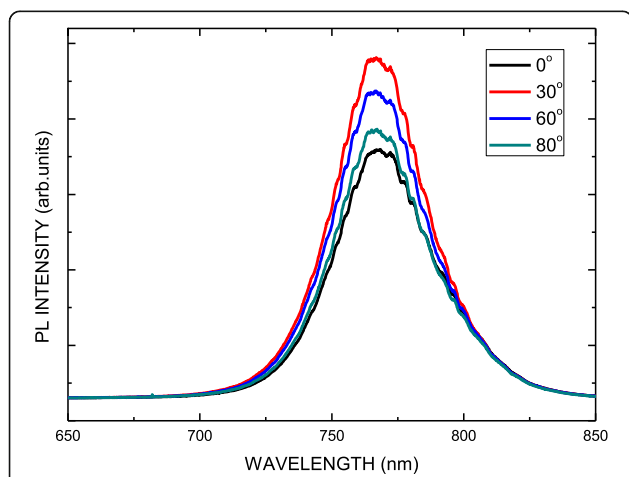


Fig. 6 PL spectra of MAPbI₃ perovskite films on PEDOT:PSS/oblique ITO layer/glass for various oblique angles

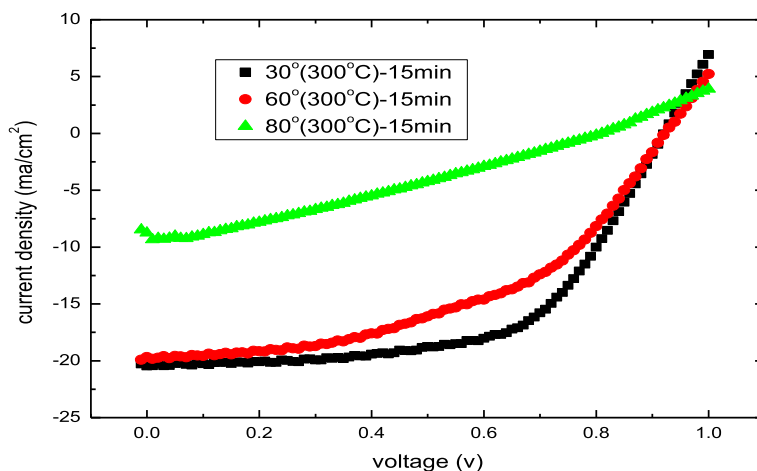


Fig. 7 Current density–voltage (J – V) of solar cells based on MAPbI₃ perovskite with oblique ITO layer sputtered at various oblique angles

stronger PL quenching effect. Therefore, ITO at an oblique angle of 80° exhibited the best exciton separation from the perovskite layer to PEDOT:PSS, owing to the favorable surface wettability of the PEDOT:PSS/oblique ITO, as shown in Fig. 4.

Figure 7 plots the current density–voltage (J – V) curve of the solar cells that are based on MAPbI₃ perovskite with an oblique ITO layer that is sputtered at various oblique angles and undergoes heat treatment at an annealing temperature of 300 °C. The sputtering time is 15 min. Table 1 presents the resulting power conversion efficiency (Eff), short-circuit current density (J_{sc}), open-circuit voltage (V_{oc}), and fill factor (FF) of the MAPbI₃ solar cells. The performance of the device degrades as the sputtering angle of the oblique ITO layer increases, because the oxygen content in the oblique ITO layers and their resistance increase with the sputtering angle [10]. Maximum efficiency can be achieved following deposition at an oblique angle of 30° owing to the favorable conductivity.

Figure 8 plots the current density–voltage (J – V) curves of the solar cells that are based on MAPbI₃ perovskite with the oblique ITO layer sputtered for various sputtering times, before undergoing heat treatment at an annealing temperature of 300 °C. Table 2 presents the corresponding power conversion efficiency (Eff), short-

circuit current density (J_{sc}), open-circuit voltage (V_{oc}), and fill factor (FF) of the MAPbI₃ solar cells. Optimum efficiency is reached when the sputtering time of the oblique ITO layer is 15 min because of the thickness of the layer and its good conductivity. The best device is obtained using this deposition angle, with J_{sc} = 20.46 mA/cm², V_{oc} = 0.92 V, FF = 60.00%, and Eff = 11.30%.

Conclusions

In summary, this work demonstrated the characteristics of MAPbI₃ perovskite films on the PEDOT:PSS/oblique-sputtered ITO/glass substrates that were fabricated using various sputtering times and sputtering angles. The device performance was optimized using an oblique ITO layer that was prepared by sputtering at 30° for 15 min, with a short-circuit current density (J_{sc}) = 20.46 mA/cm², open-

Table 1 Parameters of perovskite MAPbI₃ film on oblique ITO layer with various oblique angles

Oblique angle (°)	V_{oc} (V)	J_{sc} (mA/cm ²)	FF (%)	Eff (%)
30	0.92	20.46	60.00	11.30
60	0.922	19.68	49.11	8.91
80	0.80	8.75	31.06	2.19

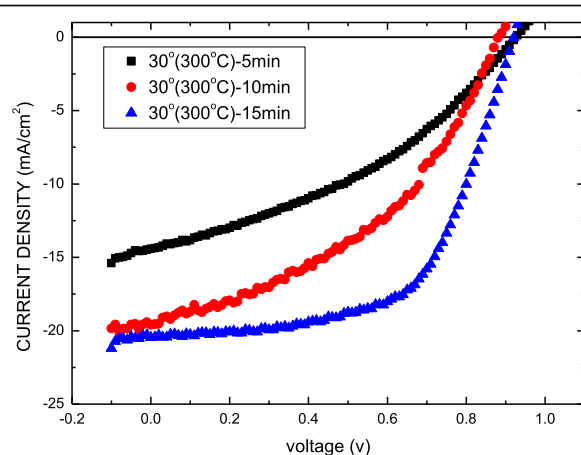


Fig. 8 Current density–voltage (J – V) of solar cells based on MAPbI₃ perovskite with oblique ITO layer sputtered for various sputtering times

Table 2 Parameters of perovskite MAPbI₃ film on oblique ITO with various sputtering times

Sputtering time (min)	V _{oc} (V)	J _{sc} (mA/cm ²)	FF (%)	Eff (%)
5	0.92	14.40	37.78	5.042
10	0.88	19.60	42.59	7.359
15	0.92	20.46	60.00	11.30

circuit voltage (V_{OC}) = 0.92 V, fill factor (FF) = 66.0%, and power conversion efficiency (Eff) = 11.3%. The performance of the device degrades as the sputtering angle of the oblique ITO layer increases from 30° to 80° because the resistance of the device increases with the sputtering angle. Although oblique ITO layers improve the scattering of incident light, the high resistivity degrades the performance of the device. Therefore, optimum efficiency can be achieved by deposition at an oblique angle of 30° owing to the conductivity.

Abbreviations

FESEM: Field-emission scanning electron microscope; GLAD: Glancing angle deposition; ITO: Indium tin oxide; J–V: Current density–voltage; MAPbI₃: CH₃NH₃PbI₃; PEDOT:PSS: Poly(3,4-ethylenedioxythiophene) polystyrene sulfonate; TCO: Transparent conductive oxide; XRD: X-ray diffractometer

Acknowledgements

The authors gratefully acknowledge the financial support from the Ministry of Science and Technology of the Republic of China under Contract No. NSC 106-2221-E-027-091.

Funding

This work was supported by the financial plan of the Ministry of Science and Technology of the Republic of China.

Authors' Contributions

KYL and LCC prepared the figures. LCC wrote the paper, designed the experiments, and analyzed the data. YJW prepared the samples and did all the measurements. LCC and KYL made the discussion and suggested the parameter. All authors read and approved the final manuscript.

Ethics Approval and Consent to Participate

Not applicable.

Competing Interests

The authors declare that they have no competing interests.

Publisher's Note

Springer Nature remains neutral with regard to jurisdictional claims in published maps and institutional affiliations.

Author details

¹Department of Electrical Engineering, China University of Science and Technology, No. 245, Sec. 3, Academia Road, Taipei 115, Taiwan.

²Department of Electro-optical Engineering, National Taipei University of Technology, 1, 3 Sec., Chung-Hsiao E. Rd, Taipei 106, Taiwan. ³Graduate Institute of Optomechatronics Engineering, China University of Science and Technology, No. 245, Sec. 3, Academia Road, Taipei 115, Taiwan.

Received: 31 August 2017 Accepted: 24 September 2017

Published online: 03 October 2017

References

1. Cui HN, Teixeira V, Meng LJ, Martins R, Fortunato E (2008) Influence of oxygen/argon pressure ratio on the morphology, optical and electrical

- properties of ITO thin films deposited at room temperature. *Vacuum* 82: 1507–1511
2. Lewis BG, Paine DC (2000) Applications and processing of transparent conducting oxides. *MRS Bull* 25:22–27
3. Limmer SJ, Cruz SV, Cao GZ (2004) Films and nanorods of transparent conducting oxide ITO by a citric acid sol route. *Appl Phys A Mater Sci Process* 79:421–424
4. Cui HN, Xi SQ (1996) The fabrication of dipped CdS and sputtered ITO thin films for photovoltaic solar cells. *Thin Solid Films* 288:325–329
5. Gorjanc TC, Leong D, Py C, Roth D (2002) Room temperature deposition of ITO using r.f. magnetron sputtering. *Thin Solid Films* 413:181–185
6. Kim SM, Rim YS, Keum MJ, Kim KH (2009) Study on the electrical and optical properties of ITO and AZO thin film by oxygen gas flow rate. *J Electroceram* 23:341–345
7. Minami T, Sonohara H, Kakumu T, Takata S (1995) Physics of very thin ITO conducting films with high transparency prepared by DC magnetron sputtering. *Thin Solid Films* 270:37–42
8. Danson N, Safi I, Hall GW, Howson RP (1998) Techniques for the sputtering of optimum indium-tin oxide films on to room-temperature substrates. *Surf Coat Technol* 99:147–160
9. Barranco A, Borras A, Gonzalez-Elipe AR, Palmero A (2016) Perspectives on oblique angle deposition of thin films: from fundamentals to devices. *Prog Mater Sci* 76:59–153
10. Chen LC, Chen CC, Sung YT, Hsu YY (2009) Oblique-angle sputtering effects on characteristics of nanocolumnar structure anisotropic indium tin oxide films. *J Electrochem Soc* 156:H471
11. Hodes G (2013) Perovskite-based solar cells. *Science* 342:317–318
12. Chen LC, Tseng ZL, Chen CC, Chang SH, Ho CH (2016) Fabrication and characteristics of CH₃NH₃PbI₃ perovskite solar cells with molybdenum-selenide hole-transport layer. *Appl Phys Express* 9:122301
13. Yang WS, Noh JH, Jeon NJ, Kim YC, Ryu S, Seo J, Seok SI (2015) High-performance photovoltaic perovskite layers fabricated through intramolecular exchange. *Science* 348:1234–1237
14. Liu M, Johnston MB, Snaith HJ (2013) Efficient planar heterojunction perovskite solar cells by vapour deposition. *Nature* 501:395–398
15. Im JH, Jang IH, Pellet N, Grätzel M, Park NG (2014) Growth of CH₃NH₃PbI₃ cuboids with controlled size for high-efficiency perovskite solar cells. *Nat Nano* 9:927–932
16. Jeon NJ, Noh JH, Yang WS, Kim YC, Ryu S, Seo J, Seok SI (2015) Compositional engineering of perovskite materials for high-performance solar cells. *Nature* 517:476–480
17. Chen LC, Tseng ZL, Huang JK (2016) A study of inverted-type perovskite solar cells with various composition ratios of (FAPbI₂)_{1-x}(MAPbBr₂)_x. *Nano* 6:183
18. Tong X, Lin F, Wu J, Wang ZM (2016) High performance perovskite solar cells. *Adv Sci* 3:5
19. Zhang Z, Wang CC, Zakaria R, Ying JY (1998) Role of particle size in nanocrystalline TiO₂-based photocatalysts. *J Phys Chem B* 102:10871–10878
20. Chang SH, Chen W-N, Chen C-C, Yeh S-C, Cheng H-M, Tseng Z-L, Chen L-C, Chiu KY, Wu W-T, Chen C-T, Chen S-H, Wu C-G (2017) Manipulating the molecular structure of PEDOT chains through controlling the viscosity of PEDOT:PSS solutions to improve the photovoltaic performance of CH₃NH₃PbI₃ solar cells. *Sol Energy Mater Sol Cells* 161:7–13
21. Bi C, Wang Q, Shao Y, Yuan Y, Xiao Z, Huang J (2015) Non-wetting surface-driven high-aspect-ratio crystalline grain growth for efficient hybrid perovskite solar cells. *Nat Commun* 6:7747
22. Lee K-M, Chen C-C, Chen L-C, Chang SH, Chen K-S, Yeh S-C, Chen C-T, Wu C-G (2017) Thickness effects of thermally evaporated C₆₀ thin films on regular-type CH₃NH₃PbI₃ based solar cells. *Sol Energy Mater Sol Cells* 164:13–18
23. Chen CC, Chang SH, Chen LC, Cheng HM, Tseng ZL, Wu CG (2016) Manipulating multicrystalline grain size in CH₃NH₃PbI₃ thin films for application in photovoltaics. *Sol Energy* 139:518–523